Measurement of a Pauli and Orbital Paramagnetic State in Bulk Gold Using X-Ray Magnetic Circular Dichroism Spectroscopy

Motohiro Suzuki,[1,*] Naomi Kawamura,[1] Hayato Miyagawa,[1] Jose S. Garitaonandia,[2]
Yoshiyuki Yamamoto,[3] and Hidenobu Hori[4]

[1]*Japan Synchrotron Radiation Research Institute (JASRI/SPring-8), 1-1-1 Kouto, Sayo, Hyogo 679-5198, Japan*
[2]*Zientzia eta Teknologia Fakultatea, Euskal Herriko Unibertsitatea, UPV/EHU, 644 pk, E-48080 Bilbao, Spain*
[3]*School of Engineering and Resource Science, Akita University, 1-1 Tegatagakuen-machi, Akita 010-8502, Japan*
[4]*School of Materials Science, Japan Advanced Institute of Science and Technology (JAIST),
1-1 Asahidai, Tatsunokuchi, Ishikawa 923-1292, Japan*

We show that bulk gold (Au) exhibits temperature-independent paramagnetism in an external magnetic field by x-ray magnetic circular dichroism spectroscopy at the Au L_2 and L_3 edges. Using the sum-rule analysis, we obtained a magnetic moment of 1.3×10^{-4} μ_B/atom in an external magnetic field of 10 T and a paramagnetic susceptibility of 8.9×10^{-6} for the $5d$ orbit. The induced paramagnetism in bulk Au is characterized by a large ($\approx 30\%$) orbital contribution. This orbital component was retained even when Au atoms formed nanoparticles, playing an important role in stabilizing the spontaneous spin polarization in the Au nanoparticles.

Gold (Au), an inert noble metal with $5d$ electrons, is known as a typical diamagnetic material with a negative magnetic susceptibility; this behavior is in contrast to the paramagnetism exhibited by other $5d$ metals, such as Pt and Ir. Au, except when in elemental form, can possess spontaneous magnetic moments when it forms alloys or layered film structures with $3d$ transition metals [1–4]. Additionally, it has been reported that Au nanoparticles (NPs) modified by some organic molecule at the surface of the cluster exhibit superparamagnetism at low temperature [5,6]. Au NPs have even been reported to exhibit ferromagnetism at room temperature [7–9]. Spontaneous magnetization in Au is presumably caused by a modification in its electronic states near the Fermi level. Previous studies have indicated the following as possible origins of magnetism in the special forms of Au: hybridization of the Au $5d$ band with the $3d$ band in a $3d$ transition metal in alloys [2] and in multilayers [3,4]; size effects; increase in the surface-to-core ratio [5]; and charge redistribution in between Au $5d$ and the electron orbitals in molecules coordinated on the cluster surface in the case of NPs [7–10]. These peculiar magnetic properties of Au have been attracting increasing attention since the discovery of magnetic Au NPs. One promising approach for elucidating the origin of magnetism in special forms of Au, particularly NPs, would be to investigate at a fundamental level the magnetism in elemental Au (i.e., parent material) in the bulk form. One of the techniques for studying weak magnetism in Au is x-ray magnetic circular dichroism (XMCD) spectroscopy [5,6,8,11]; it offers element and orbital specificity, high sensitivity to ferro- and paramagnetic moments, and no sensitivity to diamagnetic moments, in principle [12]. In this study, we used XMCD to uncover

Pauli paramagnetism in bulk Au, hidden in a diamagnetic response larger than an intrinsic paramagnetic response. We also found that a large orbital component of Au $5d$ electrons contributes to the stability of spin polarization in Au NPs.

A 5-μm-thick polycrystalline Au foil with a purity of 99.99% was used as the sample; this purity is the highest among those of commercially available foils. A synchrotron-based x-ray fluorescence analysis was performed to confirm the absence of magnetic impurities such as Fe and Co in the sample within the detection limit. The XMCD experiments were performed in the transmission mode at the beam line BL39XU at the SPring-8 synchrotron radiation facility, using x rays with a high degree of circular polarization ($P_C \geq 95\%$). An XMCD signal, $\Delta\mu = \mu^+ - \mu^-$, was the difference between the x-ray absorption coefficients for right- (μ^+) and left- (μ^-) circular polarizations and was directly taken using the helicity-modulation technique [13]. A split-type superconducting magnet was used to apply external fields of up to 10 T along the x-ray beam direction that was perpendicular to the foil plane.

Figures 1(a) and 1(c) show XMCD spectra of the sample (Au foil) at the Au L_3 ($2p_{3/2} \rightarrow 5d_{5/2}$, $6s$) and L_2 ($2p_{1/2} \rightarrow 5d_{3/2}$, $6s$) edges, respectively, measured at 10 T and a temperature of 2.3 K. In Figs. 1(b) and 1(d), the corresponding spin-averaged x-ray absorption spectroscopy (XAS) spectra, $\bar{\mu} = (\mu^+ + \mu^-)/2$, are shown; the step heights at the L_3 and L_2 edges were normalized to unity, and the XMCD data are presented as relative values to the XAS step height. We verified that the signs of the XMCD spectra were reversed for positive and negative magnetic fields of the same magnitudes, i.e., ± 10 T,
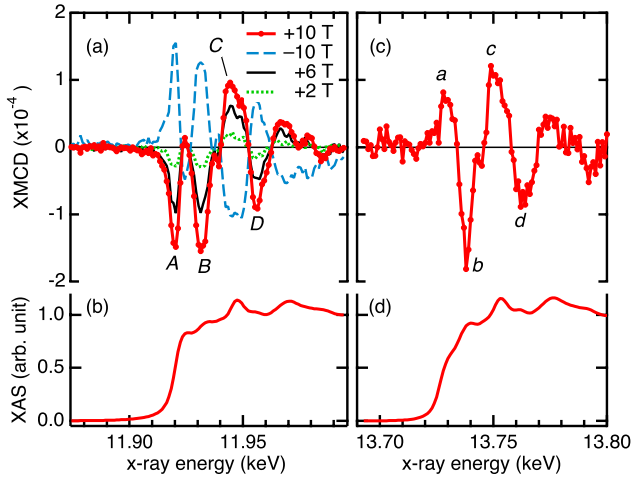
FIG. 1 (color online).   XMCD spectra of an Au foil at the Au
(a) L_3 and (c) L_2 edges, measured at 2.3 K and ± 10, $+6$, and
$+2$ T; corresponding XAS spectra at the Au (b) L_3 and (d) L_2
edges at $+10$ T.

although small systematic backgrounds ($\Delta\mu \sim 10^{-5}$) were
included in the raw data. In Fig. 1(a), the spectra for $+2$,
$+6$, and $+10$ T, after the removal of the backgrounds, are
shown to linearly change with the applied magnetic field.
The raw spectrum data measured at -10 T, containing the
nonmagnetic backgrounds, are shown to be almost an
inversion of the spectra at $+10$ T. Measurements with
opposite magnetic field direction were combined to re-
move any spurious background of nonmagnetic origin.

The measured XMCD amplitude is 10^{-4} times that of
the XAS signal, but the experiments gave clear dichroism
signals with a very high signal-to-noise ratio. The Au
XMCD signal of the foil at 10 T found in our study is 2
orders of magnitude smaller than that of Au_4Mn [1] and
$Au_{50}Fe_{50}$ alloys [2], which possess a ferromagnetic mo-
ment induced by adjacent Mn or Fe atoms, and our XMCD
signal is approximately 1/50 of Au/Co and Au/Fe multi-
layers [3,4]. We also found that our XMCD signal is 200
times smaller than that of paramagnetic Pd [1] and 10 times
smaller than that of paramagnetic Pt [14]. Thus, we suc-
cessfully detected a very small magnetic moment in bulk
Au, since XMCD amplitudes are basically proportional to
the moment of the target element.

Generally, the XMCD structure at resonance thresholds
is indicative of the magnetic states of $5d$ electrons. The
negative XMCD structure A at the L_3 edge and the positive
structure a at the L_2 edge in our study indicate that the Au
$5d$ moment is aligned parallel to the external magnetic
field. Above the resonance threshold, we observed some
oscillatory structures: B, C, and D at the L_3 edge and b, c,
and d at the L_2 edge, which extend to 70 eV above the
resonance thresholds and diminish around that energy. It is
noted that similar oscillatory structures have been observed
in the XMCD spectra of Au nanoparticles protected by
poly(allylamine hydrochloride) (PAAHC)-Au NPs [5] and

thiol-capped Au NPs [8,15]. These structures were possi-
bly formed by electric dipole transitions to the n-s and m-d
($n, m \geq 6$) bands. Although the oscillatory structures ex-
hibit XMCD amplitude comparable to the structures at the
resonance thresholds and vary linearly with the applied
magnetic field, their attributes are currently unresolved and
further investigation will be necessary. A conceivable in-
terpretation is that the structures originate from the very
strong orbital character of the higher-order empty states
because the signs of the oscillatory structures B-D and b-d
are the same in the L_3 and L_2 edges. In the following, we
focus on the structures at the resonance thresholds to
discuss the magnetic states of the $5d$ electrons in Au.

Figures 2(a)–2(e) show element-specific magnetization
curves of the sample Au foil, i.e., the plots of the amplitude
of the XMCD structure A (11.920 keV) as a function of the
magnetic field and at a temperature from 2.2 to 300 K. The
curves demonstrate the linear dependence of the XMCD on
the external field and therefore clarifiy the paramagnetic
response of bulk Au [16]. In Fig. 2(f), the slope of the
magnetization curves, $d(\Delta\mu)/dH$, a measure of magnetic
susceptibility, was shown to be independent of temperature.
Figure 3(a) shows the temperature dependence of the
XMCD spectra at the Au L_3 edge at 10 T. Clearly, the shape
and magnitude of the XMCD spectra are independent of
temperature from 2.3 to 300 K. From Fig. 3(b), it is seen that
the amplitude of the XMCD structure, A, at 2, 6, and 10 T
remains constant within the experimental error with chang-
ing temperature. On the basis of the thorough observations
that the XMCD is linearly dependent on the external mag-
netic field and independent of temperature, we presume that
bulk Au exhibits Pauli paramagnetism. Additionally, these
results deny the possibility of contamination of unexpected
paramagnetic impurities in the sample.

It is noted that the magnetic signals of the Au foil do not
originate from magnetization induced at the surface but
rather from intrinsic bulk magnetism, which is in contrast
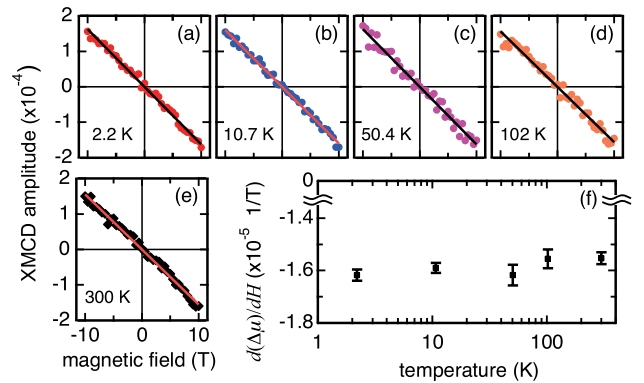
FIG. 2 (color online).   Element-specific magnetization curves
of Au foil drawn from the XMCD structure A at (a) 2.2, (b) 10.7,
(c) 50.4, (d) 102, and (e) 300 K between ± 10 T. (f) The slope
of the magnetization curves, $d(\Delta\mu)/dH$, as a function of
temperature.
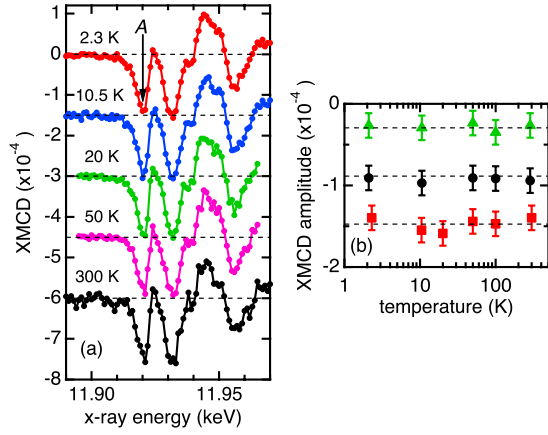
FIG. 3 (color online). (a) XMCD spectra at the Au L_3 edge, as a function of temperature at 10 T. The spectra are shown with adequate vertical offsets for better presentation, and the dashed lines show the origin of XMCD values for each spectra. (b) Amplitude of the XMCD structure, A, at 2 T (triangles), 6 T (circles), and 10 T (squares), as a function of temperature.

to the observation for Au thin films [17,18]. In our hard x-ray measurement in the transmission mode, the entire depth of the 5-μm-thick foil along the x-ray beam direction was probed. Therefore, if a surface magnetic moment would have existed and been confined to a few atomic layers at the surface of the foil, the resulting signal would have been diluted by $<10^{-3}$ owing to the large bulk-to-surface ratio and would be undetectable in the experimental scheme.

We determined the orbital and spin magnetic moments, m_{orb} and m_{spin}, respectively, from the measured XMCD spectra by the sum-rule analysis [19–21] as $m_{\mathrm{orb}} = -\frac{2}{3}(\Delta A_{L3} + \Delta A_{L2})\mu_B/C$ and $m_{\mathrm{spin}} = -(\Delta A_{L3} - 2\Delta A_{L2})\mu_B/C$, where $\Delta A_{L3} = \int_{L3} \Delta\mu(E)dE$ and $\Delta A_{L2} = \int_{L2} \Delta\mu(E)dE$ are the integrals of the XMCD spectrum at the L_3 and L_2 edges, respectively; $C = (A_{L3} + A_{L2})/h_{\mathrm{total}}$ is the ratio of the sum of the white-line integrated intensities, $A_{L3} = \int_{L3} \bar{\mu}(E)dE$ and $A_{L2} = \int_{L2} \bar{\mu}(E)dE$, after the subtraction of the contribution of the transition to the continuum, to the total 5d hole number, $h_{\mathrm{total}} = h_{5/2} + h_{3/2}$. The spin dipolar term was neglected in the case of the polycrystalline sample. To obtain the values of m_{orb} and m_{spin}, we used an approach similar to that in Refs. [22,23], where the ratio C was used instead of using separate values of $A_{L3} + A_{L2}$ and h_{total}. Using this method, one can avoid the unambiguity that can arise when subtracting the backgrounds of XAS spectra that correspond to an excitation into the continuum. Note that C is constant for the given absorption edges; its value was derived using the following equations [24]: $A_{L3} = C'(6h_{5/2} + h_{3/2})E_3/15E_2$ and $A_{L2} = C'h_{3/2}/3$, where $E_3 = 11.919$ keV and $E_2 = 13.733$ keV are the binding energies of the Au L_3 and L_2 edges, respectively. $C' = C_0N_0E_2(R_d^{2p})^2 = 7.484 \times 10^4$ eV/cm [25], which was obtained using $C_0 = 4\pi^2\alpha/3$

(here, α is the fine-structure constant); N_0 is the density of Au atoms, and R_d^{2p} is the radial dipole integral of the 2p wave function. Then, C can be expressed as

$$C = C'\frac{2}{5}\frac{E_3}{E_2}\left[1 + \frac{5}{6}\left(\frac{E_2}{E_3} - 1\right)\frac{h_{3/2}}{h_{5/2} + h_{3/2}}\right].$$

We obtained $C = 2.7 \times 10^4$ eV/cm with $h_{5/2}/h_{3/2} = 2.4$ [24,26]. The integral ΔA_{L3} (ΔA_{L2}) was determined from the XMCD intensity integrated for the first structure A (a) from 11.890 (13.701) to 11.924 (13.734) keV, reasonably chosen to include the primary contribution from 5d electrons. These two integrals were then multiplied by $\rho\Delta\sigma_{L3} = 2127$ cm^{-1} and $\rho\Delta\sigma_{L2} = 935$ cm^{-1} [27], respectively, where $\Delta\sigma_{L3}$ and $\Delta\sigma_{L2}$ are the differences in the x-ray absorption cross sections above and below the Au L_3 and L_2 edges, and ρ is the mass density of Au.

From these analyses, the spin and orbital magnetic moments of bulk Au were determined to be $m_{\mathrm{spin}} = 9.8(9) \times 10^{-5}$ μ_B/atom and $m_{\mathrm{orb}} = 2.8(3) \times 10^{-5}$ μ_B/atom, respectively, and the total magnetic moment $m_{\mathrm{spin}} + m_{\mathrm{orb}}$ was found to be $1.26(12) \times 10^{-4}$ μ_B/atom; these moments were induced in the Au 5d orbit by a magnetic field of 10 T at 2.3 K. The total moment corresponds to a paramagnetic susceptibility $\chi_{\mathrm{para}}^{5d}$ of $8.9(9) \times 10^{-6}$, based on the linear dependence of the XMCD amplitudes on an external magnetic field in Figs. 1(a) and 2(a)–2(e). The magnitude of $\chi_{\mathrm{para}}^{5d}$ is 25% that of the Au diamagnetic susceptibility, $\chi_{\mathrm{dia}} = -3.5 \times 10^{-5}$. In conventional macroscopic magnetometry, the Pauli paramagnetic response in Au is hidden by the larger diamagnetic signal. In contrast, our XMCD spectroscopy measurement successfully extracted the hidden Pauli paramagnetic response.

Table I presents a comparison between the experimental values of the paramagnetic susceptibility and the corresponding theoretical values obtained using a simple rigid-band model. If the Stoner enhancement is neglected, the Pauli paramagnetic susceptibility is expressed as $\chi_{\mathrm{Pauli}}^{5d} = 2\mu_B^2 D^{5d}(E_F)$, where $D^{5d}(E_F)$ is the partial density of states of the 5d electrons at the Fermi energy. A reported value of $D^{5d}(E_F) = 0.073$ eV^{-1} cm^{-1} by a relativistic band calculation [24] gives $\chi_{\mathrm{Pauli}}^{5d} = 5.8 \times 10^{-6}$. Thus, the experimental value of paramagnetic susceptibility, $\chi_{\mathrm{para}}^{5d} = 8.9 \times 10^{-6}$, is in reasonable agreement with the theoretical value $\chi_{\mathrm{Pauli}}^{5d}$ under the consideration of the primary contribution from the 5d electrons to the XMCD amplitude at the resonance threshold. Nevertheless, the small discrepancy remains, probably due to the orbital

TABLE I. Experimental and theoretical magnetic susceptibility values of Au.

Experimental ($\times 10^{-6}$)				Theoretical ($\times 10^{-6}$)
χ_{dia}	$\chi_{\mathrm{para}}^{5d}$	$\chi_{\mathrm{spin}}^{5d}$	χ_{orb}^{5d}	$\chi_{\mathrm{Pauli}}^{5d}$
-35	8.9(9)	6.9(6)	2.0(2)	5.8

contribution to the susceptibility [12,28]. In the analysis above, we assume a substantial density of states of the Au $5d$ electrons at the Fermi energy. A recent polarization-dependent hard x-ray photoemission study has supported a prominent $5d$ contribution to the conduction electrons [29].

We found that the induced magnetization in bulk Au has a significant orbital contribution to the susceptibility. The ratio of the orbital to spin magnetic moments was determined to be $m_{orb}/m_{spin} = 0.28 \pm 0.04$. This value is approximately 3 times $m_{orb}/m_{spin} = 0.12$ for Au in a Au/Co multilayer [3] and $m_{orb}/m_{spin} = 0.10$ in Au-capped Co NPs [23], and it is even greater than $m_{orb}/m_{spin} = 0.14$ for Au_4Mn [1] and $m_{orb}/m_{spin} \approx 0.2$ for Au-Fe alloys [2]. The observed $5d$ paramagnetic susceptibility can be resolved into spin and orbital components by using the ratio m_{orb}/m_{spin}. Then, the spin susceptibility χ_{spin}^{5d} is $6.9(6) \times 10^{-6}$ and the orbital susceptibility χ_{orb}^{5d} is $2.0(2) \times 10^{-6}$. The value of χ_{spin}^{5d} is in excellent agreement with the theoretical value of the Pauli spin susceptibility, χ_{Pauli}^{5d}. Possible contributing factors to the large orbital fraction of the paramagnetic moment could be (i) the orbital susceptibility due to spin-orbit interactions or (ii) the Kubo-Obata orbital susceptibility [28], both of which have been said to be possible contributing factors to the orbital component of the paramagnetic moment in Pd metal via XMCD study [1].

Finally, we compare the XMCD spectra of the bulk Au with those of PAAHC-Au NPs with a mean diameter 1.9 nm reported earlier [5] in Fig. 4. For the NPs, the structures A' and a' at the thresholds are more enhanced at both the L_3 and the L_2 edges than in bulk Au, whereas the structures B and b above the edge agree reasonably with those in bulk Au. The strong XMCD features confined at the thresholds suggest that the spontaneous spin polarizations of $5d$ electrons are responsible for the superparamagnetism observed in PAAHC-Au NPs [5]. By the sum-rule analysis similar to that applied to bulk Au, the orbital-to-spin magnetic moment ratio was determined for PAAHC-Au NPs. The resulting value, $m_{orb}/m_{spin} = 0.31 \pm 0.06$, reveals that the fraction of the orbital component is remarkably large in Au atoms of the NPs, which are ferromagnetically polarized, as well as paramagnetism observed in bulk Au. This large orbital contribution

probably plays a major role in stabilizing the spontaneous spin polarization in PAAHC-Au NPs [30]. Further, we emphasize that the obtained m_{orb}/m_{spin} ratios for bulk Au and Au NPs are much larger than those in systems composed of Au and $3d$ transition metals [1–3,23]. Crespo *et al.* reported that Fe impurities reduce the spontaneous magnetization of, as well as the strong local anisotropy field present at, surfaces of thiol-capped Au NPs [31]. These facts support our argument that the large orbital component observed for Au NPs is an intrinsic feature of elemental Au and it contributes to stabilizing ferromagnetic polarization. We can therefore say that the large orbital components observed in both bulk Au and Au NPs are common features of $5d$ electrons of Au and that these features possibly originate from the prominently strong spin-orbit coupling.

In conclusion, our XMCD study has demonstrated that bulk Au exhibits both Pauli and orbital paramagnetism. Our discussion relating to the XMCD results in PAAHC-Au NPs leads to one possible picture in which a large orbital component of bulk Au can be retained in the Au NPs. We speculate that this contribution is the primary origin of the spontaneous spin polarization in Au NPs, in addition to electronic hybridization and lattice strain.

FIG. 4 (color online).   XMCD spectra of PAAHC-Au NPs [5] at the Au (a) L_3 and (b) L_2 edges at 2.3 K and at 10 T, compared with the XMCD spectra of bulk Au.

*m-suzuki@spring8.or.jp

[1] A. Rogalev, F. Wilhelm, N. Jaouen, J. Goulon, and J.-P. Kappler, in *Magnetism: A Synchrotron Radiation Approach*, edited by E. Beaurepaire, H. Bulou, F. Scheurer, and J. P. Kappler, Lecture Notes in Physics Vol. 697 (Springer-Verlag, Berlin, 2006), p. 71.

[2] F. Wilhelm, P. Poulopoulos, V. Kapaklis, J.-P. Kappler, N. Jaouen, A. Rogalev, A. N. Yaresko, and C. Politis, Phys. Rev. B **77**, 224414 (2008).

[3] F. Wilhelm, M. Angelakeris, N. Jaouen, P. Poulopoulos, E. T. Papaioannou, C. Mueller, P. Fumagalli, A. Rogalev, and N. K. Flevaris, Phys. Rev. B **69**, 220404 (2004).

[4] T. Ohkochi, K. Mibu, and N. Hosoito, J. Phys. Soc. Jpn. **75**, 104707 (2006).

[5] Y. Yamamoto, T. Miura, M. Suzuki, N. Kawamura, H. Miyagawa, T. Nakamura, K. Kobayashi, T. Teranishi, and H. Hori, Phys. Rev. Lett. **93**, 116801 (2004).

[6] Y. Negishi, H. Tsunoyama, M. Suzuki, N. Kawamura, M. M. Matsushita, K. Maruyama, T. Sugawara, T. Yokoyama, and T. Tsukuda, J. Am. Chem. Soc. **128**, 12 034 (2006).

[7] P. Crespo, R. Litrán, T. C. Rojas, M. Multigner, J. M. de la Fuente, J. C. Sánchez-López, M. A. García, A. Hernando, S. Penadés, and A. Fernández, Phys. Rev. Lett. **93**, 087204 (2004).

[8] J. S. Garitaonandia, M. Insausti, E. Goikolea, M. Suzuki, J. D. Cashion, N. Kawamura, H. Ohsawa, I. Gil de Muro, K. Suzuki, F. Plazaola, and T. Rojo, Nano Lett. **8**, 661 (2008).

[9] M. Suda, N. Kameyama, M. Suzuki, N. Kawamura, and Y. Einaga, Angew. Chem., Int. Ed. Engl. **47**, 160 (2008).

[10] P. Zhang and T. K. Sham, Appl. Phys. Lett. **81**, 736 (2002).

[11] J. Stöhr and H. C. Siegmann, *Magnetism: From Fundamentals to Nanoscale Dynamics*, Springer Series in Solid-State Sciences Vol. 152 (Springer, Berlin, 2006).

[12] S. Mankovsky and H. Ebert, Phys. Rev. B **69**, 014414 (2004).

[13] M. Suzuki, N. Kawamura, M. Mizumaki, A. Urata, H. Maruyama, S. Goto, and T. Ishikawa, Jpn. J. Appl. Phys. **37**, L1488 (1998).

[14] J. Bartolomé, F. Bartolomé, L. M. García, E. Roduner, Y. Akdogan, F. Wilhelm, and A. Rogalev, Phys. Rev. B **80**, 014404 (2009).

[15] J. de la Venta, V. Bouzas, A. Pucci, M. A. Laguna- Marco, D. Haskel, S. G. E. te Velthuis, A. Hoffmann, J. Lal, M. Bleuel, G. Ruggeri, C. de Julian Fernandez, and M. A. Garcia, J. Nanosci. Nanotechnol. **9**, 6434 (2009).

[16] The negative slope in Fig. 2 implies a paramagnetic response and not a diamagnetic response because the XMCD structure A is negative for a positive field.

[17] S. Reich, G. Leitus, and Y. Feldman, Appl. Phys. Lett. **88**, 222502 (2006).

[18] M. Suda, N. Kameyama, A. Ikegami, and Y. Einaga, J. Am. Chem. Soc. **131**, 865 (2009).

[19] B. T. Thole, P. Carra, F. Sette, and G. van der Laan, Phys. Rev. Lett. **68**, 1943 (1992).

[20] P. Carra, B. T. Thole, M. Altarelli, and X. Wang, Phys. Rev. Lett. **70**, 694 (1993).

[21] H. Ebert and S. Man'kovsky, Phys. Rev. Lett. **90**, 077404 (2003).

[22] M. G. Samant, J. Stöhr, S. S. P. Parkin, G. A. Held, B. D. Hermsmeier, F. Herman, M. Van Schilfgaarde, L.-C. Duda, D. C. Mancini, N. Wassdahl, and R. Nakajima, Phys. Rev. Lett. **72**, 1112 (1994).

[23] J. Bartolomé, L. M. García, F. Bartolomé, F. Luis, R. López-Ruiz, F. Petroff, C. Deranlot, F. Wilhelm, A. Rogalev, P. Bencok, N. B. Brookes, L. Ruiz, and J. M. González-Calbet, Phys. Rev. B **77**, 184420 (2008).

[24] L. F. Mattheiss and R. E. Dietz, Phys. Rev. B **22**, 1663 (1980).

[25] M. Kuhn and T. K. Sham, Phys. Rev. B **49**, 1647 (1994).

[26] The coefficient C is rather weakly dependent on $h_{5/2}/h_{3/2}$; i.e., it varies by only $\pm 6\%$ between the extreme cases of $h_{5/2} \gg h_{3/2}$ and $h_{5/2} \ll h_{3/2}$. This dependence may cause an error, but this error would be smaller than the inherent uncertainty ($\approx 10\%$) in the sum-rule analysis.

[27] C. Chantler, K. Olsen, R. Dragoset, J. Chang, A. R. Kishore, S. A. Kotochigov, and D. S. Zucker, X-Ray Form Factor, Attenuation, and Scattering Tables, http://www.nist.gov/physlab/data/ffast/.

[28] R. Kubo and Y. Obata, J. Phys. Soc. Jpn. **11**, 547 (1956).

[29] A. Sekiyama, J. Yamaguchi, A. Higashiya, M. Obara, H. Sugiyama, M. Y. Kimura, S. Suga, S. Imada, I. A. Nekrasov, M. Yabashi, K. Tamasaku, and T. Ishikawa, New J. Phys. **12**, 043045 (2010).

[30] A. Hernando, P. Crespo, and M. A. García, Phys. Rev. Lett. **96**, 057206 (2006).

[31] P. Crespo, M. A. García, E. Fernández Pinel, M. Multigner, D. Alcántara, J. M. de la Fuente, S. Penadés, and A. Hernando, Phys. Rev. Lett. **97**, 177203 (2006).